

Scalable Substructure Discovery Algorithm For Homogeneous Multilayer Networks

Arshdeep Singh, Abhishek Santra and Sharma Chakravarthy
IT Lab and CSE Department, University of Texas at Arlington
axs9120@mavs.uta.edu, abhishek.santra@mavs.uta.edu, sharmac@cse.uta.edu

Abstract—Graph mining analyzes real-world graphs to find core substructures (connected subgraphs) in applications modeled as graphs. Substructure discovery is a process that involves identifying meaningful patterns, structures, or components within a large data set. These substructures can be of various types, such as frequent patterns, motifs, or other relevant features within the data.

To model complex data sets – with multiple types of entities and relationships – multilayer networks (or MLNs) have been shown to be more effective as compared to simple and attributed graphs. Analysis algorithms on MLNs using the decoupling approach have been shown to be both efficient and accurate. Hence, this paper focuses on substructure discovery in homogeneous multilayer networks (one type of MLN) using a novel decoupling-based approach. In this approach, each layer is processed independently, and then the results from two or more layers are composed to identify substructures in the entire MLN. The algorithm is designed and implemented, including the composition part, using one of the distributed processing frameworks (the Map/Reduce paradigm) to provide scalability.

After establishing the correctness, we analyze the speedup and response time of the proposed algorithm and approach through extensive experimental analysis on large synthetic and real-world data sets with diverse graph characteristics.

Index Terms—Homogeneous Multilayer Networks, Substructure Discovery, Decoupling approach, Accuracy & Scalability

I. INTRODUCTION

Substructure discovery is an unsupervised approach to data mining to infer new knowledge and is typically applied to graph representations. Frequent patterns are a common concept in data mining that refers to item sets, subsequences, or substructures that occur frequently in a given data set, meeting or exceeding a user-defined threshold. By identifying frequent subgraphs, we can gain insights into the underlying structure of the data and identify recurring patterns or motifs.

Graph models have been used to analyze the World Wide Web’s structure [1], social-media data, bio-informatics data [2], atoms and covalent relationships in chemistry [3], etc. Graphs are better than other data representations that embed inherent relationships among objects or entities and are also easy to understand. They use vertices and edges where each vertex of the graph will correspond to an entity and each edge is a relationship between two entities. Applications can be modeled using several graph alternatives: (i) Simple graphs, (ii) Attributed graphs, and (iii) Multilayer networks.

Need for Multilayer Networks: Social networks and many other applications often include diverse types of nodes and relationships between them. Modeling or representing them as

simple graphs (also termed a network) by using only one type of node and relationship often leads to an oversimplification of reality and information loss. Attributed graphs are better, but lack algorithms for analysis.

Sociologists have long acknowledged the significance of using distinct types of connectivity among the same group of individuals [4]. Therefore, such systems are better studied through multilayer networks.

Multilayer networks are a more general framework that allows for the analysis of complex systems with multiple interacting units and inter-dependencies that are not properly captured by simple graphs. In a multilayer network, each layer represents a different type of interaction or relationship between the system’s constituents. For example, in a social network, one layer may represent friendships between individuals, while another layer may represent professional LinkedIn connections. By analyzing the interactions between layers, it is possible to gain insights into the emergent behavior of the system as a whole.

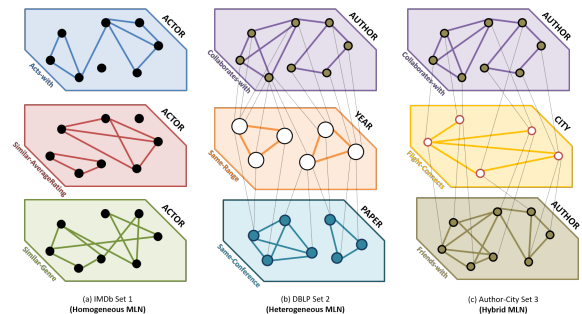


Fig. 1: MLN Types

Multilayer networks can be of several types, including (i) homogeneous (HoMLNs, Figure 1(a)), (ii) heterogeneous (HeMLNs, Figure 1(b)), and (iii) hybrid (HyMLNs, Figure 1(c)), depending on the type of layers and connections between them. Figure 1 shows these types of multilayer networks. Since the focus of this paper is HoMLNs, we start with a formal definition of a MLN.

Definition 1: A multilayer network $MLN(G, X)$, is defined by two sets of graphs. The set $G = \{G_1, G_2, \dots, G_n\}$ contains **simple** graphs (one for each layer), where $G_i(V_i, E_i)$ is defined by a set of vertices V_i and a set of edges E_i . An edge $e(v, u) \in E_i$, connects vertices v and u , where $v, u \in V_i$. The set $X = \{X_{1,2}, X_{1,3}, \dots, X_{m-1,m}\}$ consists of **bipartite**

graphs¹. Each graph $X_{i,j}(V_i, V_j, L_{i,j})$ is defined by two sets of vertices V_i and V_j and a set of edges (or links) $L_{i,j}$, such that for every link $l(a, b) \in L_{i,j}$, $a \in V_i$ and $b \in V_j$, where V_i (V_j) is the vertex set of graph G_i (G_j). Some of $X_{i,j}$ can be empty.

For HoMLNs, inter-layer graphs are implicit as nodes in layers form a common subset having same identity.

Problem Addressed: Given a homogeneous MLN (HoMLN) with l number of layers – $G_1(V, E_1), G_2(V, E_2), \dots, G_l(V, E_l)$, where V and E_i are the vertex and edge set in the i^{th} layer – the goal is to discover *interesting substructures* of the HoMLN for any r layers **correctly and efficiently** using the decoupling approach. For correctness, r HoMLN layers under consideration are conflated into a simple graph using the Boolean OR operator, and substructures discovered on that simple graph are used as the Ground Truth (GT).

Why Map/Reduce?: We have used the Map/Reduce paradigm as an example of the distributed and parallel processing approach. Without loss of generality, any other paradigm (e.g., Spark, Pregel) can be used in its stead without the need to modify the algorithms presented in this paper. Implementation will change slightly based on the choice of the framework.

Contributions of this paper are:

- **Map/Reduce Algorithm** for substructure discovery in a layer.
- **Map/Reduce Composition algorithm** to correctly generate substructures spanning Homogeneous layers.
- **Map/Reduce Partitioned approach** to layer graph processing.
- **Correctness proof** of both independent expansion and the composition algorithm (Ho-ICA).
- Extensive experimental analysis on a large number of **synthetic and real-world** graphs.
- **Accuracy** with ground truth, response time, and speedup comparisons.

Roadmap: MLN analysis alternatives are briefly discussed in Section II to highlight our choice. Section III has related work. Preliminaries and terminology are outlined in Section IV. Section V details the substructure and composition algorithm and Map/Reduce implementation of the proposed substructure discovery. Correctness of algorithms is proved in Section VI. Detailed experimental evaluation is given in Section VIII. Section IX has conclusions.

II. MLN ANALYSIS ALTERNATIVES AND CHALLENGES

Figure 2 shows three alternatives to perform analysis on MLNs. Figure 2(a) shows the traditional approach, where a MLN is conflated into a simple graph using type-independent [5] or projection-based [6] approaches. As both ignore type information for the transformation, they do not support the structure and semantic preservation of MLNs. Moreover, as observed in the literature, *without additional mappings*, these approaches are likely to result in some information loss and distortion of properties [7], or hide the

effect of different entity types and/or different intra- or inter-layer relationships [8]. At the other end of the spectrum, Figure 2(c) shows computing the result by traversing the whole MLN as a single graph. Although this has been implemented for community detection (e.g., Infomap recently, [9]), this is likely to be computationally expensive and not flexible as the number of layers and data sizes become large and new MLN algorithms need to be developed for each analysis.

Figure 2(b), on the other hand, shows an approach (termed **network decoupling**) where the analysis metric for each layer is computed independently (possibly in parallel) during the analysis (Ψ) phase **only once** and results composed using a binary operator Θ as shown in [10]–[14]. Other layer or inter-layer information is **not used** while processing a layer! This approach has been shown to be effective for Boolean operations without aggregating and losing type information. Furthermore, it has been shown to be more efficient than the approaches shown in Figure 2(a) or Figure 2(c).

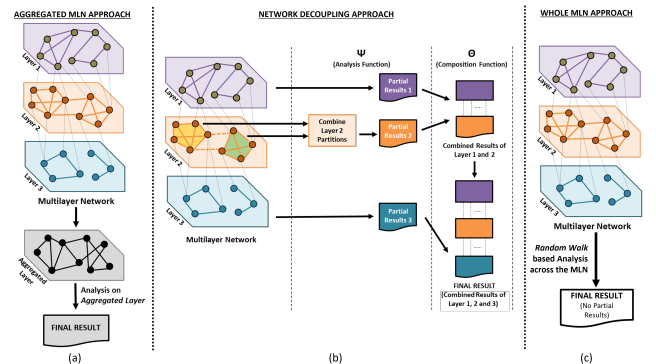


Fig. 2: Lossy (a), Decoupling (b), and MLN (c) approaches

The challenges in developing a substructure discovery algorithm are: *i) enumerating all connected subgraphs of any size in a given graph or forest (completeness), ii) identifying duplicates, if any, and remove them (soundness), iii) counting isomorphic substructures to apply the metric for each distinct substructure and ranking them, and iv) retaining top-beam substructures for the next iteration.* The enumeration is typically done by iteratively increasing the connected subgraph size by 1. Evaluation of each substructure with the desired metric (Frequency or Minimum Description Length) is carried out after each iteration. To contain the search space, a heuristic is applied to carry top-*beam* (*beam* is a parameter) results from each iteration. Current algorithms do this on a simple graph or forest. **How the decoupling approach has been adapted to the HoMLN substructure discovery is the focus of this paper and is elaborated in Section V.**

III. RELATED WORK

SUBDUE was the earliest main memory algorithm [15] developed for substructure discovery. It can perform both supervised and unsupervised substructure discovery. It uses an iterative algorithm to systematically generate larger substructures which are evaluated using Minimum Description Length (MDL [16]). SUBDUE uses the notion of a *beam* to restrict the number of substructures carried to the next iteration.

¹The number of bipartite graphs can be less or even more than the number of graphs/layers. That is, m can be \leq or even $>$ n .

AGM [17] and FSG [18] are two popular main memory graph mining algorithms that use the *a priori* concept. These approaches generate frequent $(k+1)$ subgraphs from frequent k -subgraphs. The FSG identifies repeating substructures in graphs using an *a priori* approach [18]. This is different from Subdue since it entails finding interesting substructures in a graph or forest. Canonical labeling is added to the *a priori* algorithm. The property that identical graphs have identical canonical labeling has been strategically used to identify frequent substructures. FSG determines canonical labels using a flattened graph adjacency matrix.

Disk-based graph mining algorithms [19]–[21] were developed to deal with larger graph sizes. Portions of the graph are staged into memory for processing using buffer-management techniques. Indexing was used to improve retrieval for staging. gIndex [22] uses frequent substructures as units for indexing. However, these solutions need explicit data marshalling between disk and main memory entailing developing buffer management strategies. To avoid developing complex buffer management policies, the use of relational databases has been leveraged for graph mining to leverage buffer management and query optimization. HDB-Subdue [23] used the RDBMS for graph representation and SQL to discover substructures. This approach was able to scale to handle graphs with millions of edges. However, self-joins on large relations and the number of joins needed for canonical form generation (column sorting instead of row sorting) limited scaling further.

A number of graph mining methods have shown success in cloud-based deployments [24]. Additionally, research has explored patterns in big graphs using the Map/Reduce framework [25]. However, the pattern searching technique in [25] requires a specified pattern to search for all instances of that pattern in the graph. If we need to find a pattern with the highest compressibility, we cannot supply it beforehand. Splitting/partitioning large graphs into manageable chunks for distributed processing is explored in [26]. Scalable substructure discovery on large simple graphs using Map/Reduce has been developed in [27]. A graph can be split into partitions in different ways, processed by distributed and parallel architecture, and results from across partitions combined to obtain correct results.

This paper’s focus is on MLNs instead of simple graphs, and specifically HoMLNs. Further, the decoupling-approach is chosen which entails the development of a composition function for its efficient and flexible analysis. It also uses extant substructure discovery for each layer. Correctness of the algorithm is also shown.

IV. PRELIMINARIES AND TERMINOLOGY

Edge List as graph input: A graph (layer, inter-layer, or a partition) is represented as a list of unordered edges. Each edge is completely represented by a 5-element tuple² $\langle E_l, V_{sid}, V_{sl}, V_{did}, V_{dl} \rangle$ where, E_l is edge label, V_{sid} is source vertex ID, V_{sl} is source vertex label, V_{did} is destination

²This representation is generic and can be extended to attributed graphs by using a distinct edge identifier in the edge representation. However, MLN layers are simple graphs by definition.

vertex ID and V_{dl} is destination vertex label. In this context, it is important to note that the vertex IDs (V_{sid} and V_{did}) are guaranteed to be unique. However, vertex labels (V_{sl} and V_{dl}) and the edge label (E_l) need not be unique. Table I shows the edge list representation for the input graph (or a layer) shown in Figure 3.

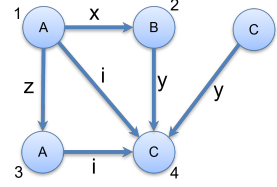


Fig. 3: Input Graph

This 5-element tuple edge representation (that includes direction) is used to represent a k -edge substructure (a connected graph with k edges and at most $k + 1$ nodes) as a collection of k 1-edge substructures. Our algorithm takes an input graph represented as a text file with a 1-edge substructure per line.

Adjacency List: Adjacency list is a representation where each vertex on which the edges are incident (both in and out) are associated with the node using a list (of 1-edge substructures.) Table II shows the edge list and adjacency list of the graph shown in Figure 3.

Edge List	Vertex ID	Adjacency List
$\langle x, 1, A, 2, B \rangle$	1	$\langle x, 1, A, 2, B \rangle, \langle z, 1, A, 3, A \rangle, \langle i, 1, A, 4, C \rangle$
$\langle z, 1, A, 3, A \rangle$	2	$\langle x, 1, A, 2, B \rangle, \langle y, 2, B, 4, C \rangle$
$\langle i, 1, A, 4, C \rangle$	3	$\langle z, 1, A, 3, A \rangle, \langle i, 3, A, 4, C \rangle$
$\langle y, 2, B, 4, C \rangle$	4	$\langle i, 1, A, 4, C \rangle, \langle y, 2, B, 4, C \rangle, \langle i, 3, A, 4, C \rangle, \langle y, 5, c, 4, c \rangle$
$\langle i, 3, A, 4, C \rangle$	5	$\langle y, 5, c, 4, c \rangle$
$\langle y, 5, c, 4, c \rangle$		

TABLE I: Edge List

TABLE II: Adjacency List

Graph Partitioning: A MLN layer L_i can be partitioned into p partitions ($L_1^i, L_2^i, \dots, L_p^i$) for distributed processing. We use *range-based partitioning* [27] to create the partitions using the vertex IDs. Each graph partition³ is a range of node IDs and the size of each partition need not be the same. There can be missing vertex IDs in a given range. As the ranges are disjoint, nodes in adjacency list partitions are also disjoint. Each vertex ID in the range and its adjacency list corresponds to a single adjacency list partition. If neighboring nodes are in two partitions, the edge connecting them will be in the adjacency list of both partitions. As a result, during expansion,

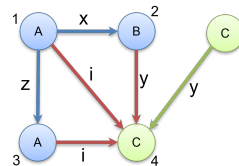


Fig. 4: Partitioned Input Graph

the same substructure can belong to many graph partitions. As adjacency list partitions are indexed on vertex IDs, each substructure is expanded only once.

Two partitions of the graph in Figure 3 are shown in Figure 4. Partition $p1$ is assigned vertex IDs from 1 to 3, whereas partition $p2$ is allotted vertex IDs 4 to 5. Both partitions are connected by red edges, which appear in different adjacency list partitions. The adjacency list partitions are displayed in table III. The edges that occur in both adjacency list partitions are $\langle i, 1, A, 4, C \rangle, \langle y, 2, B, 4, C \rangle,$ and $\langle i, 3, A, 4, C \rangle$.

³Graph partition and partition are used interchangeably. Adjacency List partition is an adjacency list for a specific graph partition.

Vertex ID	Adjacency List for Partition P1
1	(x,1,A,2,B), (z,1,A,3,A), (i,1,A,4,C)
2	(x,1,A,2,B), (y,2,B,4,C)
3	(z,1,A,3,A), (i,3,A,4,C)
Vertex ID	Adjacency List for Partition P2
4	(i,1,A,4,C), (y,2,B,4,C), (i,3,A,4,C), (y,5,c,4,c)
5	(y,5,c,4,c)

TABLE III: Adjacency Lists for Partitions

Independent Expansion of Substructures: Substructure discovery uses independent, unconstrained expansion of k -edge substructures into $(k+1)$ -edge substructures starting from an edge ($k = 1$ or a 1-edge substructure.) Each expansion of each vertex with an edge becomes a separate substructure. This independent unconstrained expansion ensures the generation of all possible substructures in a principled manner thus ensuring completeness of the substructure generation process. However, this independent expansion results in the generation of duplicate substructure instances, which must be removed to prevent incorrect counting of isomorphic substructures (soundness). Figure 5 shows how independent expansion leads to duplicates. If two substructures have the same set of vertices (with IDs) and edges (labels) and the same connectivity, they are duplicates. To ensure accurate identification of duplicates and differentiate them from isomorphic substructures, we introduce the concept of a canonical instance and canonical substructure⁴.

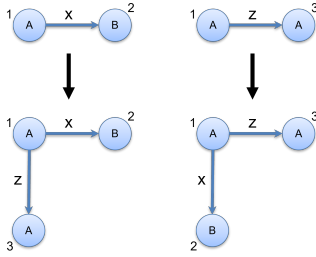


Fig. 5: Duplicate Generation

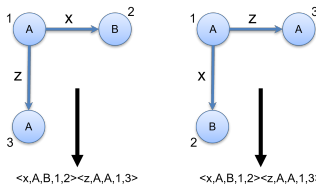


Fig. 6: Canonical Instances Example

the destination vertex IDs. Using this lexicographic order for **each 1-edge**, a substructure can be uniquely represented, which is called a canonical k -edge instance. If two k -edge substructure instances are duplicates, they must have the same ordering of their vertex IDs and therefore, will have the same canonical k -edge instance. If we convert the duplicates generated in Figure 5 to canonical instances, they will be the same, as shown in Figure 6.

⁴A canonical instance has absolute vertex IDs and a canonical substructure has relative vertex IDs.

The canonical representation of instances is helpful in identifying and removing duplicate instances. However, counting the frequency of isomorphic substructures requires a canonical form that does not rely on absolute vertex IDs. Therefore, we use a canonical form of the substructure that converts vertex IDs to relative vertex IDs.

Canonical Substructures for identifying Substructure Isomorphs: Graph isomorphism refers to the concept of two graphs being structurally identical, with a one-to-one mapping of their vertices, preserving edge connections and edge labels, and edge orientations. Exact matching of substructures is needed to compute frequent substructures accurately. Isomorphs have the same vertex labels and edge labels but different vertex IDs (as they are different instances). To identify them, we need to create a canonical substructure from the canonical instance. For this vertex IDs are changed from absolute to relative ordering. Any two exact substructures will have the same relative ordering of vertex IDs [27]. This is used to identify and compute the frequency of a substructure.

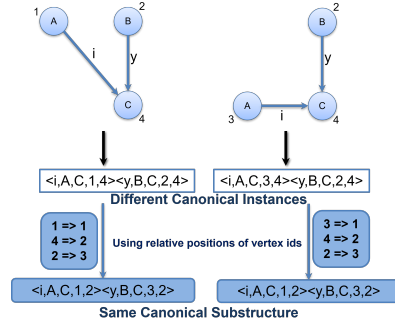


Fig. 7: Substructure Isomorphism Example

The process of canonical conversion to both instances and substructures is crucial as it enables us to identify duplicates and isomorphic instances, respectively. Thus, the canonical substructure can be derived by replacing every vertex ID with its relative position in the instance. The resulting canonical substructure allows us to identify isomorphs easily. Figure 7 provides an example of how a canonical substructure is created from the canonical instance. Note that the isomorphs have different canonical instances, but their relative positions following the canonical instance are the same. The relative positioning of vertex ID (1, 4, 2) for the first instance and (3, 4, 2) for the second instance reduces to (1, 2, 3). This leads to both having the exact same canonical substructure.

The process of canonical conversion to both instances and substructures is crucial as it enables us to identify duplicates and isomorphic instances, respectively.

A. Metrics Used for Ranking Substructures

The Minimum Description Length is an information-theoretic, domain-independent metric [15] that has been demonstrated to emphasize the significance of a substructure in terms of its ability to compress a complete graph or forest. Although it is defined, originally, in terms of bits used for graph representation, we use the number of nodes and edges for that purpose. The general formula for MDL ($DL(G)/(DL(S) + DL(G|S))$) represents the description length of the substructure S being evaluated, $DL(G|S)$ represents the description length of the graph G when compressed by replacing each instance of the

substructure S as a node, and $DL(G)$ (or $DL(S)$) represents the description length of the original graph (or the substructure S). The substructure of the graph achieves the highest compression when the MDL value is the highest. Both the frequency of the subgraph and its connectivity have an impact on compression. The frequency of substructures can also be used as a metric as used in FSG and others.

V. ARCHITECTURE AND COMPOSITION ALGORITHM

Instead of a single network, we have multiple layers and the goal is to find *interesting* substructures in the MLN (across all layers). Substructures in a Multilayer Network (MLN) can exist in different ways: i) can exist solely in one layer (intra-layer substructure) or ii) can span multiple layers (inter-layer substructure). An algorithm exists for detecting substructures within a graph or a layer. For scalability, this algorithm has been extended to use range-based partitions and generate substructures across partitions correctly [27]. Hence, our primary focus is on generating all inter-layer substructures correctly during the composition phase so MDL (or some other metric) can be applied to rank the MLN substructures.

Below we present the **Iterative Composition Algorithm (Ho-ICA)** for **Homogeneous** MLNs which performs composition *after each iteration*. That is, substructures for each participating layer are generated during an iteration and the generated layer substructure instances are used for composing **missing** inter-layer substructures. After that, duplicate elimination is done for generated instances using canonical representation and substructures are counted using canonical substructures to apply MDL. This process repeats after each iteration until the substructure discovery algorithm terminates and outputs the best substructures based on the given parameters.

As inter-layer substructures are composed in every iteration, our conjecture is that this approach should not have any accuracy drop (if done correctly) as all substructures (intra and inter) are generated in each iteration and evaluated using the metric before keeping the *top-beam* substructures for the next iteration. We will validate this conjecture experimentally. We will also provide the operational correctness of the algorithm. Although we may be adding an extra step of computation (composition) as compared to the ground truth computation, yet the efficiency (as compared to ground truth) will improve by an order of magnitude while preserving accuracy, as we are dealing with smaller graphs that can be processed in parallel.

We will experimentally evaluate the developed algorithm for correctness, efficiency, and scalability. We will also discuss how distributed processing resources can be matched to the input graph size to keep the desired response time.

A. Ho-ICA: HoMLN Iterative Composition Algorithm

Figure 8 provides a comprehensive diagrammatic overview of Ho-ICA for substructure discovery for a HoMLN.

This approach generates substructures for each layer in each iteration, converts them to canonical instances, and eliminates duplicates. Composition algorithm is applied at the end of layer substructure generation in each iteration to generate

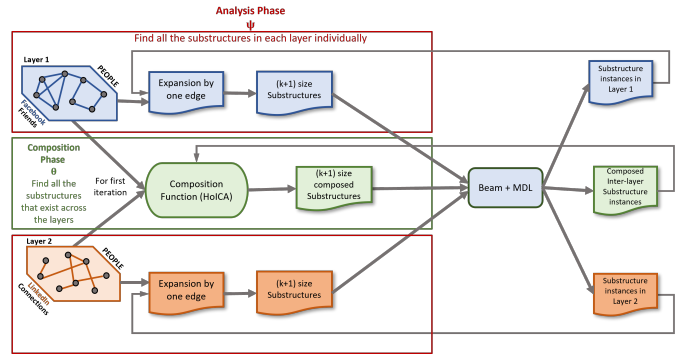


Fig. 8: Decoupling Approach Overview for Iterative Composition

missing inter-layer substructures. After that, all substructures from the individual layers and composed substructures spanning layers (after duplicate elimination) are aggregated. They are converted into canonical substructures for applying a ranking metric (such as MDL) to generate the *top-beam* substructures for the next iteration. Each iteration corresponds to a particular size of substructure. In each iteration, the substructures are expanded by a single edge in their own layer, starting with size one substructures (an edge) for the first iteration. This generates all the intra-layer substructures for that size. Also, in the first iteration which generates 2-edge substructures, the composition function generates inter-layer substructures by expanding instances from each layer using the adjacency list of other layers. In subsequent iterations, composition function will generate composed substructures of size $k+1$, using the composed substructures from the previous iteration (size k).

At the end of each iteration, the substructures from each layer and the inter-layer substructures are separated for the next iteration. This is critical for the decoupling principle which stipulates that layers are processed independently and without using the knowledge of the other layers. In the next iteration, substructures from each layer are expanded by an edge from that layer and in the next composition stage, intra-layer substructures are expanded using edge from the other layer and inter-layer substructures are expanded with one edge from either layer and the process repeats. Note that composition can make use of information from both layers.

The input of the Ho-ICA algorithm is a set of composed substructures from the previous iteration, each of size $k-1$, where k is at least 2. We then expand these substructures using adjacency lists of other layers, to get inter-layer composed substructures of size k . The inter-layer substructures, in addition to the intra-layer substructures generated in the current iteration, are forwarded to the metric evaluation process followed by beam application. Given that the beam substructures now consist of both intra-layer and inter-layer substructures, they are separated (to be consistent with the decoupling philosophy) and sent to their respective tasks for the next iteration. Algorithm 1 describes the composition function used to compose substructures after each iteration.

The algorithm expands each previously generated inter-layer substructure using adjacency lists of all layers (line 3).

Algorithm 1 Ho-ICA: Iterative Composition Algorithm

Require: (S_{k-1}) : Set of all substructures of size $k-1$ from previous iteration (composed and layers), where k is at least 2 represented as a sequence of edges $\langle e_1, \dots, e_k \rangle$, where e_i is 5-element tuple; $AL_p^m \dots AL_p^n$: Adjacency List partitions for N layers

Ensure: Composed inter-layer substructures of size k

```
1: for each  $(k-1)$  edge instance  $I_{k-1} \in (S_{k-1})$  do
2:   for each vertex-ID  $v \in I_{k-1}$  do
3:      $EL_v \leftarrow \{v \in AL_p^m \cup \dots \cup AL_p^n\}$ 
       {edge list of  $v$  from every layer}
4:     for each edge  $e \in EL_v$  do
5:       if  $e \notin I_{k-1}$  then
6:          $I_k^{composed} \leftarrow I_{k-1} + e$ 
           {Append edge  $e$  in lexicographical order}
7:          $S_k^{composed} \leftarrow I_k^{composed}$ 
           {Add to composed set  $S_k^{composed}$ }
8:       end if
9:     end for
10:  end for
11: end for
```

VI. CORRECTNESS OF APPROACH

In this section, we will prove that expanding each substructure instance of a graph or forest one edge at a time followed by duplicate elimination is complete and sound. Completeness means *all* substructures that should be generated for evaluation are generated without fail. Soundness means that *only* those substructures that should be generated are generated. We need duplicate elimination for soundness. In addition, we will also argue that the composition algorithm presented here is operationally correct and will generate all inter-layer substructures without fail. We will also prove the correctness of the presented Ho-ICA algorithm.

A. Correctness of Independent Substructure Expansion

Given a forest F of graphs, let $G(V, E)$ be an arbitrary connected graph⁵ in F , where V is the set of nodes and E is the set of edges (directed or undirected). An adjacency list exists for F which is indexed on node ID and its value being the edges incident on that node (directed and undirected). Let AL_F be the adjacency list of F .

Let g be a connected substructure instance of G with k edges and at most $k+1$ nodes⁶. Let n' be a node in g and d' be its degree in g . Let the degree of n' in G be d . *Independent expansion refers to each substructure instance of size k (i.e., k edges) being expanded without considering any other substructure of size k .*

Lemma 6.1: *Independent expansion of the substructure instance g generates all instances that should be generated from g .*

Proof: During independent expansion, an arbitrary node n' of g is expanded by one edge (along with the connected node) that is not already present in the substructure instance,

⁵Without loss of generality, the results extend to all connected components in F . As our layers are simple graphs/forest, we are not considering multiple edges between nodes, and loops.

⁶It is easy to see that the first iteration on an edge using the adjacency list generates all 2 edge substructures containing that edge.

but is incident on n' in the graph G . This edge is added to the subgraph instance g increasing the number of edges (and may be nodes) by 1. It also increases the degree of the node n' by 1 and increases the size of the substructure by 1. This becomes a new substructure instance with at most $k+2$ nodes and $k+1$ edges. This is done for each edge incident on n' in G that is not in g . For node n' , the number of such 1-edge expansions will be $(d-d')$. This process is repeated for all nodes in g and *separate* substructure instances are generated for each expansion. The total number of substructure instances generated for each substructure instance g depends on the degree of individual nodes in g and the degree of corresponding nodes in G . This is repeated for all substructure instances of size k in iteration k generating all substructure instances of size $(k+1)$ in k^{th} iteration. Therefore, as each node in g is expanded to the fullest extent, this process will generate all possible substructure instances of size $(k+1)$ of graph G in iteration k , that should be generated from g . ■

Lemma 6.2: *In the absence of any constraints, the application of Lemma 6.1 repeatedly on substructure instances starting with the substructures of size 1 achieves completeness.*

Proof: The above process starts with 1-edge substructure instances (essentially all edges of graph G). In iteration 1 all substructure instances of size 2 are generated using the above procedure. This process is repeated on increasing substructure instances until no more expansion can be performed. The final substructure instance generated with unconstrained expansion is G itself. This expansion until no more instances can be generated achieves completeness. ■

Note that independent expansion of a single substructure instance only generates distinct instances. However, when two different substructure instances are expanded independently, duplicate instances may be generated. An example of this has been shown in Figure 5. Instances at the bottom were generated by expanding on different substructure instances at the top by an edge. The resulting substructures become identical in node IDs and labels as well as edge labels as can be seen after the canonical ordering. Only one needs to be kept and the other eliminated for soundness. We have indicated earlier how canonical form of substructures are used for identifying duplicate instances for elimination.

Lemma 6.3: *Independent expansion of instances of G with duplicate elimination at the end of each iteration achieves soundness.*

Proof: Consider all subgraph instances of size k . When these are expanded independently in the k^{th} iteration, a large number of instances of size $(k+1)$ are generated. As indicated above, there may be duplicate instances among them. By converting each substructure to its canonical form and sorting them, duplicates are brought together. Duplicates are eliminated by keeping only one instance. This ensures soundness. ■

Theorem 6.4: *Independent expansion of instances followed by duplicate elimination in each iteration is complete and sound.*

Proof: Follows directly from Lemmas 6.2 and 6.3. ■

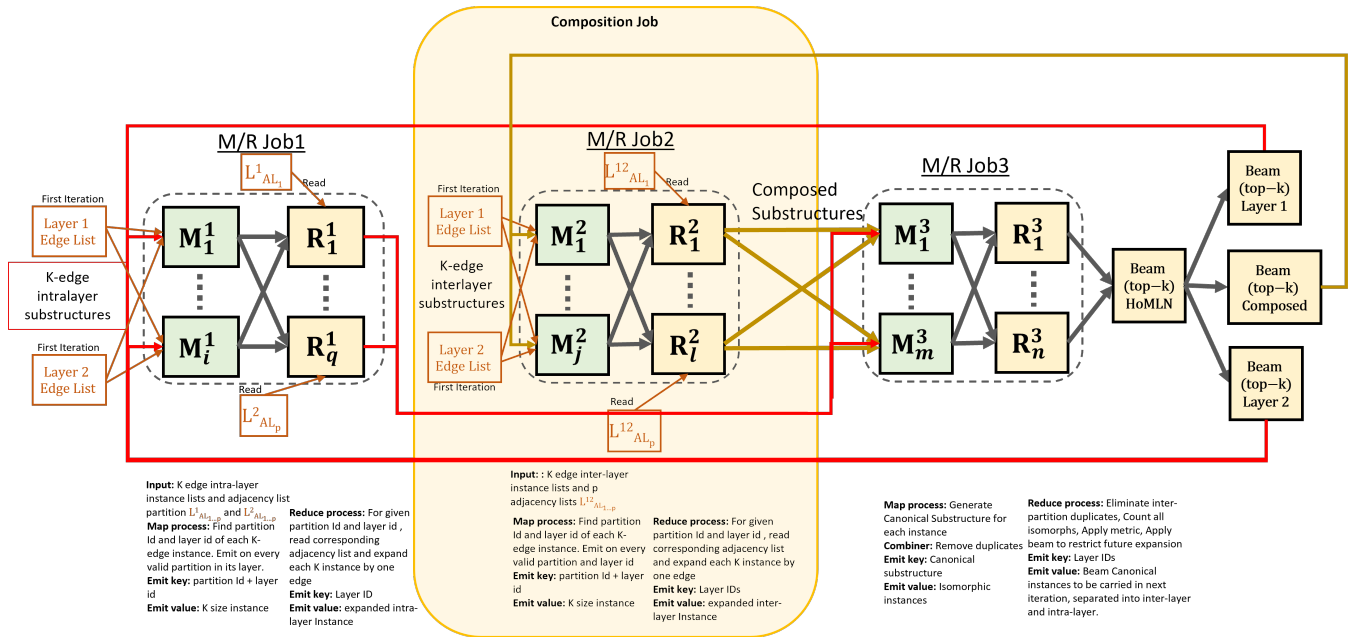


Fig. 9: Ho-ICA Architecture using Map/Reduce

B. Correctness of the Ho-ICA Algorithm

Here we need to show that Ho-ICA algorithm generated **all** inter-layer instances without fail. Note that intra-layer instances are correctly generated, as established by Theorem 6.4.

We will use proof by induction. We will show that for any iteration k , Ho-ICA correctly generates all results for the next iteration $(k + 1)$. Following is the proof:

Lemma 6.5: For any iteration i , the Ho-ICA algorithm correctly generates all inter-layer instances.

Proof: Base Case: For iteration 1, Ho-ICA uses size 1 substructures (i.e., the edge list) of each layer and generates size 2 inter-layer substructure instances using the adjacency lists of the other layers. As it utilizes all edges in each layer to pair with edges from any other layer, the Ho-ICA will generate every size 2 inter-layer instance. With duplicate elimination all size 2 distinct inter-layer substructures are generated. Thus, Ho-ICA correctly generates all size 2 substructure instances in the first iteration correctly.

Inductive Case: We assume that for some arbitrary iteration $k-1$, the algorithm has correctly generated all inter-layer substructure instances of size k .

In iteration k , Ho-ICA will expand inter-layer substructure instances from the previous iteration (iteration $k-1$) to generate expanded inter-layer substructure instances. Specifically, it employs the appropriate adjacency list for each layer to which the to be composed instance belongs. Through an unconstrained expansion on every vertex ID of the instance using these adjacency lists, Ho-ICA ensures the generation of all possible expanded inter-layer instances. For two layers L_1 and L_2 ,

- 1) all intra-layer substructures are generated by expanding L_1 substructures using L_2 adjacency list and L_2 substructures using L_1 adjacency list.
- 2) inter-layer substructures are generated using composed substructures from the previous iteration and expanding

them using both L_1 and L_2 adjacency lists.

After the unconstrained expansion, duplicate elimination is done to ensure soundness. Thus, Ho-ICA accurately generates all instances for the iteration k using all instances from iteration $k - 1$. ■

VII. IMPLEMENTATION USING MAP/REDUCE

In this section, we discuss the implementation of the decoupling-based iterative substructure discovery algorithm (Ho-ICA) discussed in Section V. We use the Map/Reduce framework to leverage distributed and parallel processing. Both range partitioning and substructure discovery have been implemented using the Map/Reduce framework.

The iterative composition algorithm for substructure discovery in HoMLNs follows the two distinct phases of the decoupling approach, namely, analysis and composition phases. Figure 9 shows the overall flow of Ho-ICA using Map/Reduce.

The algorithm comprises three Map/Reduce jobs for each iteration. The first pair generates layer substructure instances using independent and unconstrained expansion. The third pair counts substructures, applies MDL, and generates *top-beam* substructures for the next iteration. The composition function Ho-ICA is encapsulated in the second Map/Reduce pair. The composition function will now expand inter-layer composed instances by using the adjacency list as explained in Algo. 1. As shown, only iteration 1 is different from the rest.

VIII. EXPERIMENTAL EVALUATION AND VALIDATION

Experiments were conducted on the Expanse cluster at SDSC (San Diego Supercomputer Center), details shown in Table IV.

Data Set Generation: In the context of our substructure discovery algorithm, when we model a data set as a HoMLN, each layer is considered as an independent graph. Consequently, we can transform a large simple graph into a

Compute Node Component	Configuration
Node Count	728
Cores/Node	128 built on 2 processors (64 cores each)
Processor	AMD EPYC 7742
Memory	256 GB DDR4 DRAM
Storage	1TB Intel P4510 NVMe PCIe SSD

TABLE IV: Expanse System Details

MLN by partitioning it into layers. This approach provides the flexibility to assess the algorithm’s performance across MLNs of varying sizes while maintaining control over other graph characteristics, such as the edge distribution among layers. Furthermore, for empirical validation, we can embed substructures with known frequencies to ensure consistent identification of substructures and their frequency whether the data set is processed as a single graph or as a MLN. Hence, our methodology involves generating substantial single graphs with embedded substructures, followed by the creation of layers for the HoMLN.

Data Set	Used For	Beam Value	M/R configs (per layer)
Synthetic	Accuracy, Response Time	4,8,12	2M/2R, 4M/4R, 8M/8R
Synthetic Large	Response Time, Scalability	4	4M/4R, 8M/8R, 16M/16R, 32M/32R
Amazon	Response Time, Scalability	4	8M/8R, 16M/16R, 32M/32R, 64M/64R
LiveJournal	Response Time, Scalability	4	8M/8R, 16M/16R, 32M/32R, 64M/64R

TABLE V: Data Set Description

Base Graph #nodes, #edges	GID	Edge Dist.	#L1 edges	#L2 edges
50KV, 100KE	1	50/50	49797	50203
	2	70/30	69862	30138
	3	90/10	89899	10101
100KV, 500KE	4	50/50	249953	250047
	5	70/30	349722	150278
	6	90/10	449691	50309
400KV, 1000KE	7	50/50	500006	499994
	8	70/30	700077	299923
	9	90/10	899994	1000006
1000KV, 4000KE	10	50/50	1998995	2001005
	11	70/30	2799577	1200423
	12	90/10	3599822	4001178
Amazon .74MV, 2.6ME	13	50/50	1305431	1305160
	14	70/30	1827821	782770
	15	90/10	2349423	261168
LiveJournal 4.9MV, 69ME	16	50/50	34489570	34504203
	17	70/30	48295818	20697955
	18	90/10	62096307	6897466

TABLE VI: Data Sets with Edge Distributions

Data Set Description: We conducted experiments on real-world and synthetic data sets to evaluate the effectiveness, correctness, speedup concerning different configurations of mappers and reducers, and scalability of our approach. Table V outlines the data sets used. We have utilized synthetic graphs of various sizes with multiple embedded substructures

of known frequency. This helps us to verify our results. Additionally, real-world data sets from Amazon [28], [29] and LiveJournal [30] were also used for our experiments.

For these data sets, diverse two-layer HoMLNs were generated with three edge distributions (50/50, 70/30, and 90/10 choosing edges randomly) for testing, details in Table VI.

A. Empirical Correctness

To verify the correctness of our algorithms, we conducted tests on small synthetic graphs generated by Subgen with sizes ranging from 50KV/100KE to 1MV/4ME with predefined embedded substructures. **Subdue [15] and Ho-ICA when run on these graphs, consistently discovered the same substructures and frequency.**

B. Accuracy

As indicated above, Ho-ICA consistently exhibited full accuracy, a validation further supported by our experimental analyses. To verify the correctness on large graphs, we embedded substructures of known size and frequency to test the correctness of the proposed approach. Across various synthetic data sets, Ho-ICA also consistently identified all instances of the embedded substructure correctly with exact frequencies.

1) *Effect of Layer Distribution on Accuracy:* Ho-ICA consistently attains full accuracy regardless of the layer distribution, displaying resilience to variations in the distribution ratio — be it 50/50, 70/30, or 90/10.

2) *Effect of Beam on Accuracy:* Ho-ICA is able to consistently achieve full accuracy at a beam size of 4 (default value). Thus, increasing beam size further will not have any effect on accuracy except more computation is involved.

3) *Effect of Layer Connectivity on Accuracy:* This experiment was to make sure Ho-ICA correctly identifies interesting substructures whether the layer graph is connected or not. Again, Ho-ICA displayed full accuracy even when the layer graph was disconnected. This is consistent with the correctness proof in Section VI.

C. Response Time and Scalability: Synthetic Graphs

To validate speedup using distributed processing, we varied the number of partitions of the same graph along with increasing the number of mappers and reducers to maximize parallelization. The objective was to observe how response time varies when resources are increased. This will also indicate the speedup we can achieve (linear trend or exhibits diminishing returns). Large synthetic and real-world data sets were utilized to verify the speedup and scalability of our approach.

1) *Synthetic Graphs:* To analyze the speedup achieved on synthetic data sets, various data set sizes were explored - 50K vertices and 100K edges (50KV100KV), 100K vertices and 500K edges (100KV500KE), 400K vertices and 1 million edges (400KV1ME), and 1 million vertices and 4 million edges (1MV4ME). Regardless of the layer size, each layer was partitioned into the same number of partitions. We experimented with 8, 16, 32, and 64 partitions, maintaining an equal number of mappers and reducers. We saw a similar trend in

each data set. Here, we have focused on the largest data set, 1MV4ME. Results for all data sets are shown in Fig. 14 (b).

For Ho-ICA, Fig. 10 reveals a speedup of at least **48.32%** as we increased the number of partitions and the numbers of mappers/reducers from 8 to 16. Subsequently, a speedup of at least **43.49%** was observed when further increasing them from 16 to 32. Finally, a speedup of at least **34.41%** was noticed when further increasing them from 32 to 64. However, the speedup achieved was not linear; doubling the mappers and reducers does not halve the time taken. As the number of partitions increases, the overhead of writing more files and shuffling comes into effect.

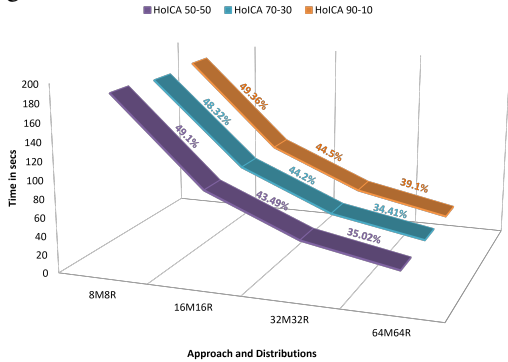


Fig. 10: Speedup Analysis: 1MV4ME Data Set

This observed speedup can be attributed to the more partitions of the graphs, processed by an increased number of processors in parallel. Smaller-sized partitions contribute to a reduced computational load on each processor, leading to higher speedup. However, the diminishing speedup suggests that increasing the number of partitions does not continuously improve performance. Higher number of partitions allows more instances to belong to multiple partitions, increasing the potential for inter-partition duplication. This leads to redundant work in different processors. Moreover, excessively small input splits can negatively impact Hadoop performance, introducing overhead related to task setup, communication, and coordination. Conversely, overly large input splits can result in an uneven distribution of processing workload among nodes, leading to inefficient resource utilization. Hence, determining the optimal number of input splits is crucial for optimizing Hadoop job performance. If the objective is to maximize efficiency, employing 16 Mappers/Reducers appears to be the most effective choice as it provides the best speedup. However, in case there is surplus processing power available, 64 Mappers/Reducers still yield a respectable speedup of around 30% while taking the least amount of time.

2) *Effect of Layer Distribution:* As evident from Figure 10, layer distribution does not significantly impact the efficiency of Ho-ICA. This behavior stems from the algorithm's implementation, where all layers are processed within the same Map/Reduce job, enabling effective load balancing and ensuring uniform load distribution among processors.

D. Response Time and Scalability: Real-World Graphs

We have also employed real-world graphs to demonstrate scalability and speedup as the characteristics of a real-world graph

may be quite different from that of a synthetically generated graph. Two real-world data sets - Amazon and LiveJournal - were used with sizes of 0.74MV2.6ME and 4.9MV69ME, respectively. These data sets were partitioned into 8, 16, 32, and 64 partitions, and experiments were performed using same number of mappers and reducers for each.

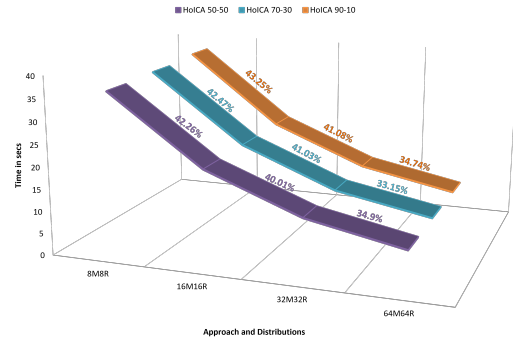


Fig. 11: Speedup Analysis: Amazon Data Set

Amazon (0.74MV2.6ME): The speed in Figure 11, is very similar to the speed up seen for synthetic graphs. Across distributions, we observe speedups of at least **42.26%**, **40.01%** and **33.15%** going from 8 to 16, 16 to 32, and 32 to 64 mappers/reducers, respectively.

As the focus of this paper is on the composition algorithm, its correctness, and implementation using Map/Reduce, Figure 12 shows only the composition time for the Amazon data set. Note that there were no embedded substructures as this is a real-world data set. From Figure 12, it can be seen that composition takes most time in iteration 1 and is almost flat for other iterations. This is because, in iteration 1, **all** edges are composed whereas in subsequent iterations, only *top-beam* substructures are composed.

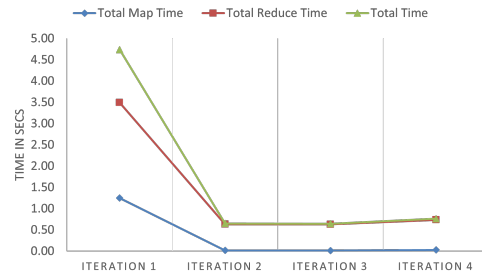


Fig. 12: Composition Job for Amazon Data Set

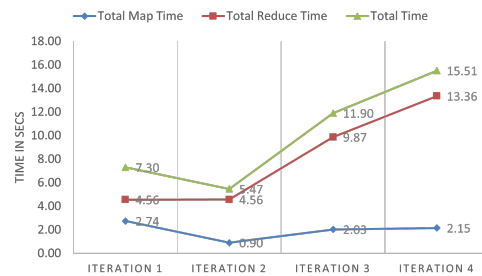


Fig. 13: Composition Job for 1MV4ME Data Set

On the other hand, in Figure 13 the same composition time is displayed for the synthetic data set 1MV4ME. As this data set has an embedded substructure of size 5, iterations 3

and 4 see an increase in composition time as compared to iterations 1 and 2. Larger substructures (in higher iterations) have more vertex IDs that they can be expanded on, requiring more computational work. This leads to a steady increase in the reduce time from iteration 2 onwards as expansion is done in the reducer. The map time only slightly increases, as the mapper solely handles the routing of substructures based on vertex IDs. This implies that the map time is solely dependent on the number of substructure instances received by the mapper, irrespective of their size. It is essential to note that the dip from iteration 1 to iteration 2 is due to the beam being applied after the first iteration. In other words, all the edges in the graph are processed in the first iteration, but only the top beam substructures are processed starting from the second iteration. This greatly reduces the number of substructures considered for expansion. Thus, a significant dip is observed between iteration 1 and iteration 2.

LiveJournal (4.9MV69ME): Here, trends are similar to those seen in the Amazon data set. This data set is **notably larger at 4.9 Million Vertices and 69 Million Edges** than the previous data sets. The average speedup while varying the number of partitions and mappers/reducers is greater than that observed in the Amazon data set.

Specifically, a consistent decrease of nearly **50%** is observed in transitions from 8 to 16 and 16 to 32 partitions. However, from 32 to 64 partitions, the speedup diminishes to 39%, but it remains higher compared to other data sets. This can be attributed to the larger size of the graph, which helps alleviate the added overhead from adding more tasks/processors. Having a large overhead due to a higher number of tasks for a small data set would diminish the speedup, but for a sufficiently large data set like LiveJournal, doubling the processors results in nearly double speedup (*approx. 50% reduction in time*).

E. Response Time for All Experiments Performed

Figure 14 shows all the experiments that were performed for all the data sets shown in Table VI.

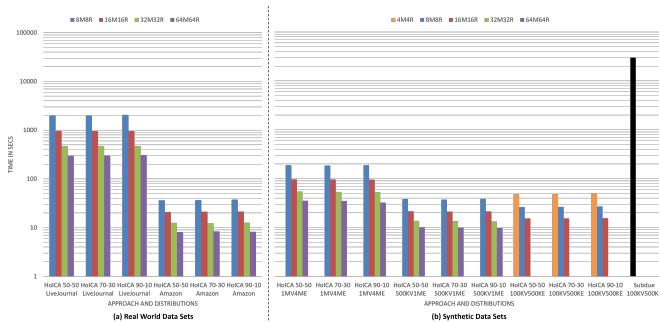


Fig. 14: Comprehensive SpeedUp Experiment Results

IX. CONCLUSIONS AND FUTURE WORK

This paper introduces a scalable algorithm for substructure discovery for HoMLNs, using a decoupling-based strategy. A

composition algorithm was presented and implemented using Map/Reduce, demonstrating its correctness and scalability.

Future work includes further improving efficiency by skipping composing after each iteration, still preserving accuracy. This seems to be a challenge as it is a trade-off among efficiency, accuracy, and graph characteristics.

REFERENCES

- [1] A. P. F. Miguel E. Coimbra and L. Veiga, "An analysis of the graph processing landscape," *Journal of Big Data*, 2021.
- [2] N. G. de Bruijn, "A combinatorial problem," *Proc. Akad. Wet. Amsterdam*, vol. 49, pp. 758–764, 1946.
- [3] A. T. Balaban, "Applications of graph theory in chemistry," *Journal of Chemical Information and Computer Sciences*, vol. 25, no. 3, pp. 334–343, 1985. [Online]. Available: <https://doi.org/10.1021/ci00047a033>
- [4] S. Wasserman and K. Faust, *Social network analysis: Methods and applications*. Cambridge university press, 1994.
- [5] M. D. Domenico, V. Nicosia, A. Arenas, and V. Latora, "Layer aggregation and reducibility of multilayer interconnected networks," *CoRR*, vol. abs/1405.0425, 2014.
- [6] A. Berenstein, M. P. Magarinos, A. Chernomoretz, and F. Aguerro, "A multilayer network approach for guiding drug repositioning in neglected diseases," *PLOS*, vol. 10, no. 1, p. e0004300, 2016.
- [7] M. Kivelä, A. Arenas, M. Barthelemy, J. P. Gleeson, Y. Moreno, and M. A. Porter, "Multilayer networks," *CoRR*, vol. abs/1309.7233, 2013.
- [8] M. De Domenico, A. Solé-Ribalta, S. Gómez, and A. Arenas, "Navigability of interconnected networks under random failures," *Proc. of Ntl. Acad. of Sciences*, 2014.
- [9] J. D. Wilson, J. Palowitch, S. Bhamidi, and A. B. Nobel, "Community extraction in multilayer networks with heterogeneous community structure," *J. Mach. Learn. Res.*, vol. 18, no. 1, pp. 5458–5506, 2017.
- [10] A. Santra, F. A. Irany, K. Madduri, S. Chakravarthy, and S. Bhowmick, "Efficient community detection in multilayer networks using boolean compositions," *Frontiers Big Data*, vol. 6, 2023. [Online]. Available: <https://doi.org/10.3389/fdata.2023.1144793>
- [11] A. Santra, S. Bhowmick, and S. Chakravarthy, "Efficient community re-creation in multilayer networks using boolean operations," in *International Conference on Computational Science, ICCS 2017, 12-14 June 2017, Zurich, Switzerland*, ser. *Procedia Computer Science*, P. Koumoutsakos, M. Lees, V. V. Krzhizhanovskaya, J. J. Dongarra, and P. M. A. Sloot, Eds., vol. 108. Elsevier, 2017, pp. 58–67. [Online]. Available: <https://doi.org/10.1016/j.procs.2017.05.246>
- [12] H. R. Pavel, A. Roy, A. Santra, and S. Chakravarthy, "Closeness centrality detection in homogeneous multilayer networks," in *Proceedings of the 15th International Joint Conference on Knowledge Discovery, Knowledge Engineering and Knowledge Management, IC3K 2023, Volume 1: KDIR, Rome, Italy, November 13-15, 2023*, A. L. N. Fred, F. Coenen, and J. Bernardino, Eds. SCITEPRESS, 2023, pp. 17–29. [Online]. Available: <https://doi.org/10.5220/0012159500003598>
- [13] K. Mukunda, A. Roy, A. Santra, and S. Chakravarthy, "Stress centrality in heterogeneous multilayer networks: Heuristics-based detection," in *IEEE Ninth International Conference on Big Data Computing Service and Applications, BigDataService 2023, Athens, Greece, July 17-20, 2023*. IEEE, 2023, pp. 103–110. [Online]. Available: <https://doi.org/10.1109/BigDataService58306.2023.00021>
- [14] A. Santra, K. S. Komar, S. Bhowmick, and S. Chakravarthy, "From base data to knowledge discovery - A life cycle approach - using multilayer networks," *Data Knowl. Eng.*, vol. 141, p. 102058, 2022. [Online]. Available: <https://doi.org/10.1016/j.datak.2022.102058>
- [15] D. J. Cook and L. B. Holder, "Substructure discovery using minimum description length and background knowledge," *Journal of Artificial Intelligence Research*, vol. 1, pp. 231–255, 1994.
- [16] J. Rissanen, "A Universal Prior for Integers and Estimation by Minimum Description Length," *The Annals of Statistics*, vol. 11, no. 2, pp. 416 – 431, 1983. [Online]. Available: <https://doi.org/10.1214/aos/1176346150>
- [17] R. Agrawal and R. Srikant, "Fast Algorithms for Mining Association Rules," in *Very Large Data Bases*, 1994, pp. 487–499.
- [18] M. Deshpande, M. Kuramochi, and G. Karypis, "Frequent Substructure-Based Approaches for Classifying Chemical Compounds," in *IEEE International Conference on Data Mining*, 2003, pp. 35–42.

- [19] J. Pei, J. Han, B. Mortazavi-Asl, H. Pinto, Q. Chen, U. Dayal, and M.-C. Hsu, "PrefixSpan.: mining sequential patterns efficiently by prefix-projected pattern growth," in *ICDE*, 2001, pp. 215–224.
- [20] H. Bunke and K. Shearer, "A graph distance metric based on the maximal common subgraph," *Pattern Recognition Letters*, vol. 19, pp. 255–259, 1998.
- [21] S. Alexaki and V. C. et al., "On Storing Voluminous RDF Descriptions: The Case of Web Portal Catalogs," in *Intl. Workshop on the Web and Databases*, 2001, pp. 43–48.
- [22] X. Yan, P. S. Yu, and J. Han, "Graph indexing: a frequent structure-based approach," in *Proceedings of the 2004 ACM SIGMOD international conference on Management of data*, 2004, pp. 335–346.
- [23] S. Padmanabhan and S. Chakravarthy, "Hdb-subdue: A scalable approach to graph mining," in *DaWaK*, 2009, pp. 325–338.
- [24] S. Suri and S. Vassilvitskii, "Counting triangles and the curse of the last reducer," in *World Wide Web Conference Series*, 2011, pp. 607–614.
- [25] Y. Liu, X. Jiang, H. Chen, J. Ma, and X. Zhang, "MapReduce-Based Pattern Finding Algorithm Applied in Motif Detection for Prescription Compatibility Network," in *Advanced Parallel Programming Technologies*, 2009, pp. 341–355.
- [26] S. Yang, X. Yan, B. Zong, and A. Khan, "Towards effective partition management for large graphs," in *SIGMOD Conf.*, 2012, pp. 517–528.
- [27] S. Das and S. Chakravarthy, "Partition and conquer: Map/reduce way of substructure discovery," in *International Conference on Big Data Analytics and Knowledge Discovery*. Springer, 2015, pp. 365–378.
- [28] P. Boldi, M. Rosa, M. Santini, and S. Vigna, "Layered label propagation: A multiresolution coordinate-free ordering for compressing social networks," in *Proc. of the 13th WWW Conference*, 2011, pp. 587–596.
- [29] P. Boldi and S. Vigna, "The WebGraph framework I: Compression techniques," in *Proc. of the 13th WWW Conference*, 2004, pp. 595–601.
- [30] Live-journal. [Online]. Available: <http://snap.stanford.edu/data/com-LiveJournal.html>.